Processed dietary fiber partially hydrolyzed guar gum increases susceptibility to colitis and colon tumorigenesis in mice

Check for updates

Sangshan Tian[1], Umesh K. Goand[1], Devendra Paudel[1], Giang V. Le[1], Amit K. Tiwari[2], K. Sandeep Prabhu[3] & Vishal Singh[1,4] ✉

The vital role of naturally occurring dietary fibers (DFs) in maintaining intestinal health has fueled the incorporation of refined DFs into processed foods. The present study assessed the impact of purified DF partially hydrolyzed guar gum (Phgg) on intestinal inflammation and colitis-associated colon carcinogenesis (CAC). Surprisingly, wild-type mice fed Phgg exhibited more severe dextran sulfate sodium (DSS)-induced colitis than the control group. Additionally, Phgg feeding led to increased colonic expression of genes promoting cell proliferation. Accordingly, extensive colon tumorigenesis was observed in Phgg-fed mice in the azoxymethane (AOM)/DSS model, whereas the control group exhibited no visible tumors. Mice fed low-Phgg (2.5%) diet exhibited more colitis and tumorigenesis than controls, but less than those on regular Phgg diet (7.5%), suggesting a dose-dependent influence of Phgg on colitis and CAC development. Our study reveals that Phgg supplementation exacerbates colitis and promotes colon tumorigenesis, warranting further investigation into the potential gastrointestinal health risks associated with processed Phgg consumption.

Colorectal cancer (CRC) is the third-leading cause of cancer-related deaths in the United States, posing a significant public health challenge[1]. According to the data from Global Cancer Observatory, ~1.9 million new cases of CRC were diagnosed worldwide in 2022[2]. Over 95% of CRCs are adenocarcinomas. The transformation of an intestinal polyp into cancer occurs through the adeno-to-carcinoma sequence, a series of genetic changes involving proto-oncogene mutations and altered expression of tumor suppressor and cell survival genes that promote tumor growth[3]. Factors contributing to CRC include aging, genetic predisposition, environmental influences, and prolonged intestinal inflammation[4]. Colitis-associated colorectal cancer (CAC) is defined as a form of CRC that is commonly seen in patients with inflammatory bowel disease (IBD). Prolonged colonic inflammation significantly increases the risk of CAC compared to healthy individuals[5,6]. Although the detailed molecular pathways remain underexplored, the IBD patients displaying chronic, hyperactive immune responses are at an elevated risk of developing CAC[5]. Higher consumption of fiber-rich whole foods, such as fruits and vegetables, improve overall well-being, including gastrointestinal health[7]. Dietary Guidelines for Americans recommend increasing fiber intake primarily from whole and minimally processed foods. Since only about 10% of Americans meet their dietary recommendation of fruits and vegetables[8], incorporating isolated dietary fibers (DFs) into processed foods presents a potential strategy to meet their daily intake. This approach, in fact, is marketed as enhanced nutritional value of these foods and to help meet fiber intake.

DFs are edible complex carbohydrates that are resistant to human digestion. DFs are broadly classified into insoluble and soluble based on their solubility in water. Insoluble fibers like cellulose are generally resistant to fermentation by gut bacteria in both humans and mice. Despite limited bacterial breakdown, they offer various health benefits, including increased stool bulk and a laxative effect[9]. Soluble DFs, such as inulin and partially hydrolyzed guar gum (Phgg), are readily fermented by both human and murine gut microbiota. These soluble DFs also offer numerous benefits to the host's metabolic and gastrointestinal (GI) health[10]. Improvements in intestinal health markers, such as enhanced gut barrier function[11], reduced

[1]Department of Nutritional Sciences, The Pennsylvania State University, University Park, PA, USA. [2]Department of Pharmaceutical Sciences, College of Pharmacy, University of Arkansas for Medical Sciences, Little Rock, AR, USA. [3]Department of Veterinary and Biomedical Sciences, The Pennsylvania State University, University Park, PA, USA. [4]One Health Microbiome Center, Huck Institutes of the Life Sciences, The Pennsylvania State University, University Park, PA, USA. ✉e-mail: vxs28@psu.edu

levels of pro-inflammatory cytokines[12], and increased colonic cell proliferation[13–15], upon consuming these soluble DFs, primarily stemmed from interventional studies conducted in cohorts of healthy rodents and human populations. Whether DF supplementation exerts similar effects during ongoing intestinal inflammation remains largely unknown and has begun to be unraveled recently. These recent studies have produced conflicting results regarding the impact of refined DFs on intestinal health. A subset of these studies suggests beneficial effects on intestinal inflammation[16–19] while another subgroup raises concerns about potential adverse effects on both intestinal inflammation and colon tumorigenesis[20–24]. A comprehensive evaluation of refined DFs that are being incorporated into the ultra-processed food and promoted as supplements is necessary to determine their impact on intestinal health, especially during periods of ongoing inflammation. In this study, we evaluated Phgg, a soluble DF widely used in the food industry as a food thickener and emulsifier[25], and available as a supplement, on colonic inflammation and the markers of cell survival and proliferation. Additionally, we evaluated the effect of Phgg on colon tumorigenesis using a colitis-associated colon cancer model[26].

Results

Diet containing refined Phgg exacerbates colonic inflammation

Since a subset of patients with IBD reports heightened inflammation after consuming certain DF[20], we examined the effect of processed DF Phgg on colitis in a mouse model of acute colitis. WT mice, 1 week post-weaning, were maintained on a Phgg-containing diet (7.5% w/w Phgg, 2.5% w/w cellulose) or a control diet (10% w/w cellulose) for 4 weeks. Subsequently, mice were divided into two groups receiving either regular water (no treatment, NT) or dextran sulfate sodium-containing water (DSS; 1.4% w/v) for 7 days (Fig. 1a). Although no significant differences were found in the body weight among the NT groups, Phgg-fed mice challenged with DSS lost ~15% more weight than the control-DSS group (Fig. 1b). Furthermore, shortened colon length and increased spleen weights were observed in Phgg-DSS group compared to rest of the groups (Fig. 1c–e). Histological analysis demonstrated epithelial damage, loss of crypt structure, and immune cell infiltration within the submucosal layer in DSS-challenged mice maintained on Phgg (Fig. 1fi). The Phgg-fed group also exhibited a substantial loss of goblet cells and reduced mucin 2 secretion compared to the control group in the DSS-intervention group. (Fig. 1fii, iii). In line, mice in the Phgg-DSS group showed significant elevation in both colonic and systemic lipocalin 2 (Lcn2), a biomarker of colonic inflammation, and serum amyloid A (SAA) (Fig. 1g–i). Remarkably, Phgg feeding in the experimental group without colitis displayed comparable levels of intestinal health markers, including mucin expression and immune markers. This suggests that Phgg supplementation alone does not adversely impact intestinal health but fuels ongoing inflammation and worsens colitis.

Phgg supplementation alters colonic immune markers favoring inflammation

To determine the factors that worsened colonic inflammation in the Phgg-fed group, we measured the expression of chemokines and cytokines in the colon. Increased colonic mRNA expression of monocyte chemoattractant protein 1 (Mcp1) and C-X-C motif chemokine ligand 1 (Cxcl1) in Phgg-fed mice treated with DSS (Fig. 2a, b) suggested increased infiltration of immune cells. This was evidenced in H&E-stained sections, which revealed extensive inflammatory cell infiltration in the colonic mucosa and submucosa compared to DSS-treated controls. In line, we observed elevated mRNA transcripts of the pro-inflammatory markers inducible nitric oxide synthase (iNos) and interleukin 6 (Il-6) specifically in the Phgg+DSS group compared to the remaining groups (Fig. 2c, d). The expression of tumor necrosis factor alpha (Tnfα) remained unaltered across the groups (Fig. 2e). Most notably, the mRNA levels of anti-inflammatory cytokines Il-4 and Il-10 were augmented in the DSS-treated control group but not in the Phgg+DSS group (Fig. 2f, g). In fact, the Phgg+DSS group displayed reduced colonic expressions of Il-4 and Il-10. The colonic mRNA expression data

suggest that Phgg supplementation not only promoted the expression of pro-inflammatory molecules but also reduced the levels of anti-inflammatory molecules.

IL-6 is considered both an intestinal immune activity modulator and a tumorigenesis promoter[27,28]. The proliferative and survival effects of IL-6 are largely mediated by signal transducer and activator of transcription 3 (STAT3)[29]. Intriguingly, the colonic mRNA level of Stat3 was exclusively augmented in the Phgg+ DSS group (Fig. 2h). We further examined colonic protein levels of the pleiotropic cytokine IL-6, the chemokine CXCL1, the pro-inflammatory cytokine IL-1β, and its physiological antagonist, the IL-1 receptor antagonist (IL1Ra), via ELISA. We found increased colonic levels of IL-6, CXCL1, and IL-1β in the Phgg+ DSS group compared to the DSS-treated control (Fig. 2i–k). IL1Ra inhibits inflammation mediated by IL-1β by blocking its binding to its receptor, IL-1R1. Therefore, to assess the IL-1β activity, we examined the colonic IL-1β/IL1Ra ratio, which was markedly elevated in the DSS-treated Phgg-fed group (Fig. 2l, m), suggesting heightened IL-1β-mediated immune activity in this group. In support, we also observed increased colonic expression of Lcn2 (assessed via immunohistochemical staining) in the DSS-challenged Phgg-fed group (Fig. S1). Altogether, these data indicate an imbalanced intestinal inflammatory milieu arising from elevated pro-inflammatory factors and reduced anti-inflammatory cytokines, which contributed to exacerbating colitis in the Phgg-fed group.

Phgg induces aberrant expression of intestinal barrier function and cell proliferation markers

Tight junction (TJ) proteins maintain the intestinal barrier integrity, protecting against gut microbial invasion[30] and regulating the mucosal repair[31,32]. Thus, colonic mRNA transcripts of TJ proteins were assessed. Among the barrier-forming claudins (Cldn1, 4, 5, and 7), the mRNA level of Cldn1 was significantly elevated in the Phgg+ DSS group (Fig. 3a). This finding aligns with human IBD specimens, which exhibited increased CLDN1 in ulcerative colitis (UC) colon compared to non-disease colon[33]. Concurrently, we observed reduced colonic expression of Cldn7 (Fig. 3d), whose deficiency is shown to increase susceptibility to colitis and associated colon tumorigenesis[34–36]. The colonic levels of Cldn4 and Cldn5 remain unaltered across the groups (Fig. 3b, c). Next, we examined the colonic expression of pore-forming claudins, Cldn2 and Cldn10. Phgg-fed mice displayed an increased level of Cldn2[37] in the colitis group (Fig. 3e). Data from mucosal biopsy specimens from human patients with UC show a similar pattern, with low CLDN2 expression in normal colon and an increase in CLDN2 in mucosal specimens from patients with UC[38]. Another pore-forming claudin, Cldn10[39] exhibited an increasing trend in the Phgg+ DSS group, although the data did not reach statistical significance (Fig. 3f). The expression of E-cadherin[40], which regulates the incorporation of claudins into TJs, was comparable across all four groups (Fig. 3g). We next evaluated the zonula occludens (ZO −1, −2, and −3)—ZOs are membrane-associated cytosolic scaffolding proteins that facilitate assembly of TJ proteins, including claudins[41]. Among the three ZO types (Zo1-3) examined, only the expression of Zo1 was significantly altered (decreased) in mice challenged with DSS. However, no significant difference in Zo1 expression was observed between the control and Phgg-fed groups maintained on DSS (Fig. 3h–j).

Subsequently, we evaluated the expression of genes related to cell proliferation and survival. Proliferating cell nuclear antigen (PCNA) is a critical DNA repair protein during DNA replication, and its overexpression is correlated with colorectal carcinoma progression and metastasis[42]. We observed increased colonic expression of Pcna specifically in Phgg-fed mice that received DSS (Fig. 4a), suggesting increased cell proliferation. Relative to control, the tumor-suppressing protein p53 and its effector protein, p53 upregulated modulator of apoptosis (Puma), exhibited significantly decreased expression with Phgg consumption (Fig. 4b, c). However, their mRNA transcripts remained unchanged in inflammatory conditions induced by DSS.
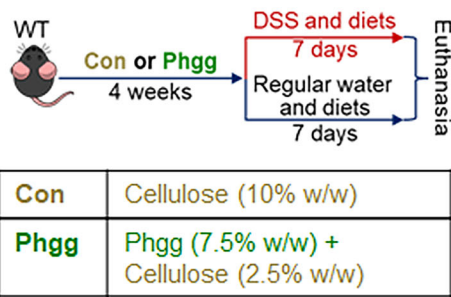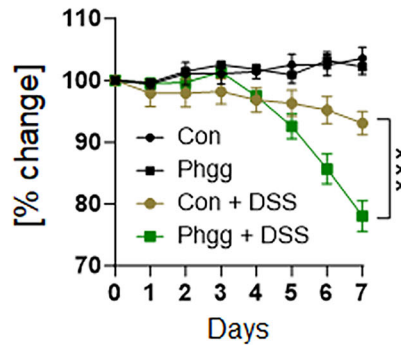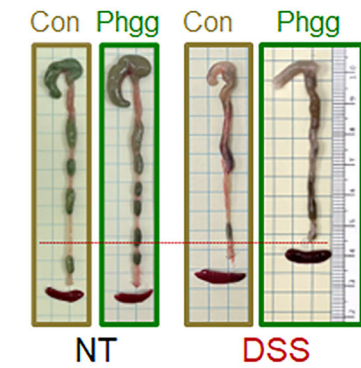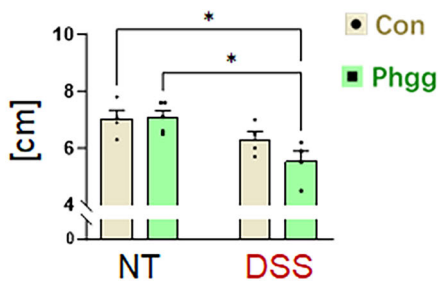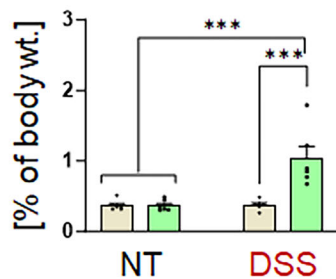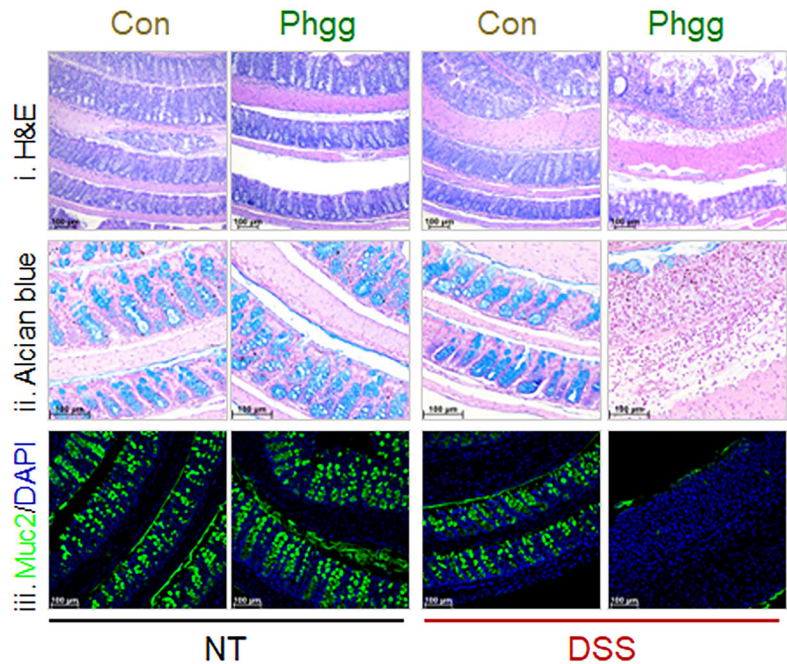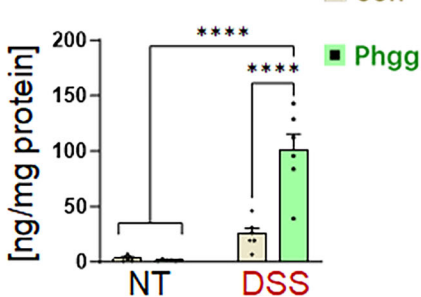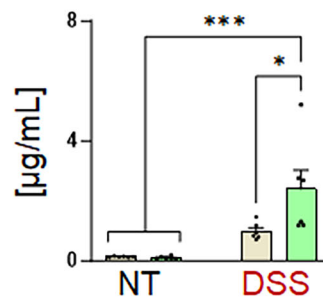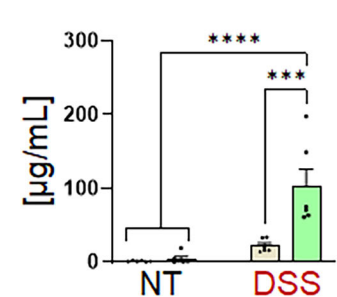
Fig. 1 | Phgg exacerbates DSS-induced colitis. (**a**) Experimental layout. (**b**) Percent change in body weight (b. wt.) during the DSS-intervention period. (**c**) Representative gross colon images. (**d**) Colon length. (**e**) Spleen weight (as a percent of the b. wt. on euthanasia day). (**f**) Representative images of (i) H&E-stained (original magnification, ×50), (ii) alcian blue-stained colon sections (original magnification, ×100), and (iii) immunohistochemical staining for mucin 2 (Muc2; green), with DAPI (blue) to visualize the nucleus (original magnification, ×50). (**g**) Colon Lcn2. Serum levels of (**h**) Lcn2 and (**i**) SAA Values are presented as mean ± SEM (**b, d, e, g–i**). $*p < 0.05$, $**p < 0.01$, $***p < 0.001$, and $****p < 0.0001$.
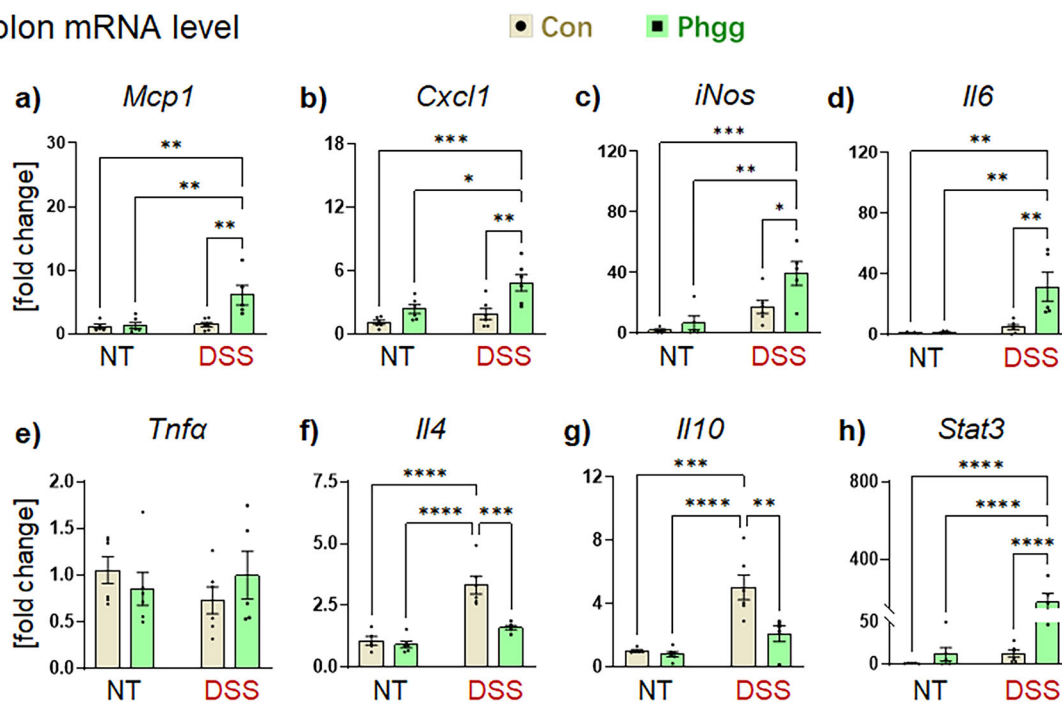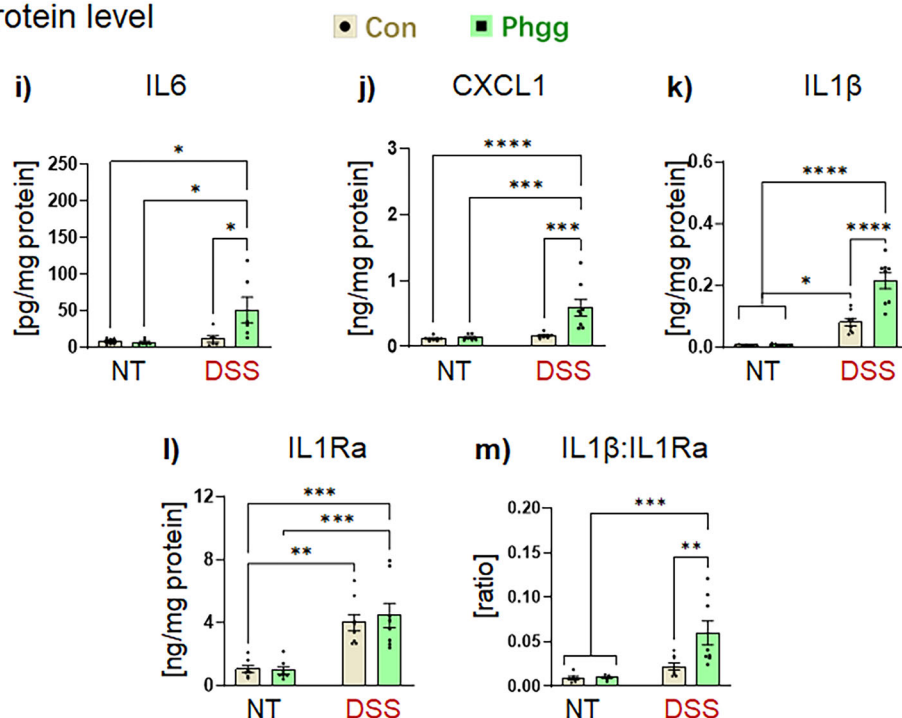
Fig. 2 | Phgg-fed group displays increased pro- and reduced anti-inflammatory markers upon DSS intervention. The colonic tissue was obtained from no treatment (NT) and DSS-intervention (DSS) groups and analyzed for mRNA expression (via qPCR) and protein level (via ELISA). **a** *Monocyte chemoattractant protein 1* (*Mcp1*), (**b**) *CXC motif chemokine ligand 1* (*Cxcl1*), (**c**) *Inducible nitric oxide synthase* (*iNos*), (**d**) *Interleukin 6* (*Il-6*), (**e**) *Tumor necrosis factor alpha* (*Tnfα*), (**f**) *Il-4*, and **g** *Il-10*. **h** *Signal transducer and activator of transcription 3* (*Stat3*). **i**–**m** Protein level was estimated via ELISA and normalized by total colon protein concentration. **i** IL-6, (**j**) CXCL1, (**k**) IL-1β, (**l**) IL1 receptor antagonist (IL1Ra), and **m** IL-1β to IL1Ra ratio. Values are presented as mean ± SEM. $*p < 0.05$, $**p < 0.01$, $***p < 0.001$, and $****p < 0.0001$.

Alongside, the colonic mRNA level of *caspase3*, a potent inducer of apoptosis, was reduced in the Phgg-DSS group compared to the Con-DSS group (Fig. 4d). The mRNA levels of cell survival-related genes such as *cyclin D1*, B-cell lymphoma 2 (*Bcl2*), and myeloid leukemia 1 (*Mcl1*) remained unaltered across all groups (Fig. 4e–g). Collectively, these results indicate that Phgg distinctively alters the colonic expression of genes favoring barrier dysfunction and cell proliferation, particularly in the inflamed environment.
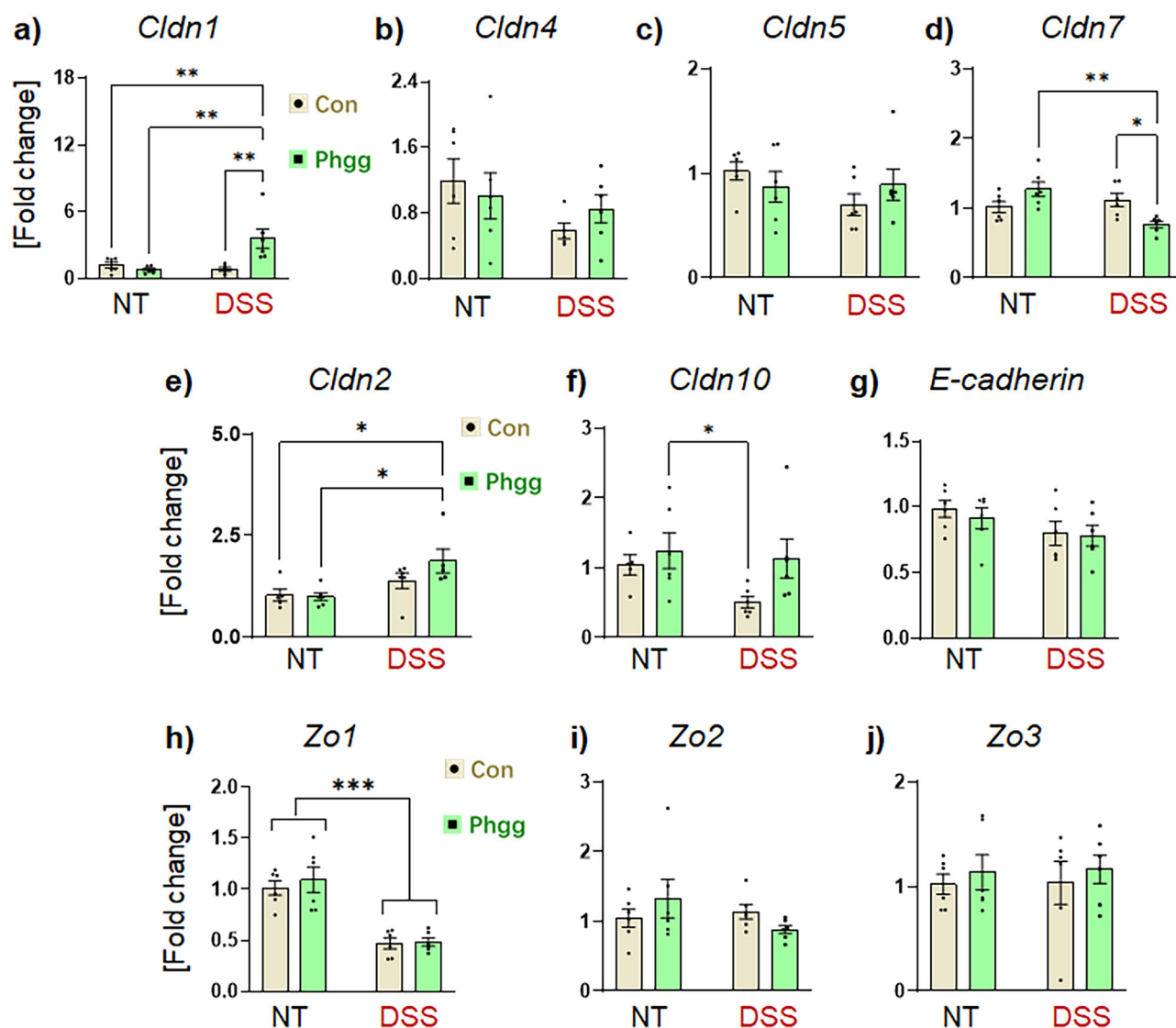
Fig. 3 | Phgg-fed mice exhibit differential gene expression of tight junction proteins in the colon. The expression of tight junction proteins was estimated at the mRNA level via qPCR in colon tissues. **a** *Claudin-1* (*Cldn1*), (**b**) *Cldn4*, (**c**) *Cldn5*, (**d**) *Cldn7*, (**e**) *Cldn2*, and **f** *Cldn10*. **g** *E-cadherin*. **h** *Zonula occludes 1* (*Zo1*), (**i**) *Zo2*, and **j** *Zo3*. Values are presented as mean ± SEM. *$p < 0.05$ and **$p < 0.01$.

Phgg promotes colitis-associated colon tumorigenesis in both male and female mice

As demonstrated in the previous section, the Phgg-fed group displayed a distinctive increase in the chemokines and cytokines linked with colon carcinogenesis. Additionally, we observed elevated expression of cell proliferation markers and reduced levels of tumor suppressor and antiapoptotic genes. Therefore, we hypothesized that Phgg supplementation may potentiate CAC development. To test this, WT male mice were fed either a control or Phgg-containing diet for 4 weeks and then received a single injection of AOM (7.5 mg/kg body weight). After 1 week, colonic inflammation was instigated with 1% DSS, followed by two additional cycles of 0.75% w/v DSS (Fig. 5a). Since Phgg-fed mice developed extensive colitis even at a reduced dose of DSS (1.4% w/v), we used an even lower dose of DSS in the AOM/DSS model. Despite using the very low dose of DSS, the Phgg group exhibited a substantial loss of body weight particularly during DSS administration phase (Fig. 5b). Most notably, 3 out of 7 (~43% of total number) Phgg-fed mice succumbed to death due to severe colitis disease (Fig. 5c). All surviving mice on Phgg diets developed colon tumors, while no visible tumor was found in the control groups (Fig. 5d, e). To further investigate the significant finding that only Phgg-fed mice developed colon

tumors, we conducted histochemical staining in colon sections. Histological examination revealed that colon tumors in the distal colon regions of Phgg-fed groups exhibit characteristics of adenocarcinoma (Fig. 5f)[43]. Additionally, we observed a significant increase in nuclear translocation of β-catenin in the tumor regions compared to the control group (Fig. 5g–h). Interestingly, the adjacent non-tumor regions of the Phgg-fed groups also exhibited a moderate increase in β-catenin nuclear localization compared to the control group, suggesting a potential predisposition to tumorigenesis. Such increased nuclear β-catenin suggests activation of the Wnt-β-catenin signaling pathway[44] upon Phgg feeding. Surprisingly, expression of Ki67, a cell proliferation marker[45], was reduced in the tumor regions compared to adjacent normal tissue in the Phgg group and the control group (Fig. 5g–i). This finding aligns with previous studies demonstrating that reduced Ki67 expression is associated with later stages of CRC[46] and lower survival rates[47]. Immunohistochemical staining for Lcn2, a marker of intestinal inflammation, in colonic tissue displayed an increasing trend in Lcn2 expression in AOM/DSS-challenged Phgg-fed groups, indicating a state of ongoing intestinal inflammation (Fig. S2).

To mechanistically understand how Phgg supplementation induced extensive colon tumorigenesis, we subsequently examined the expression
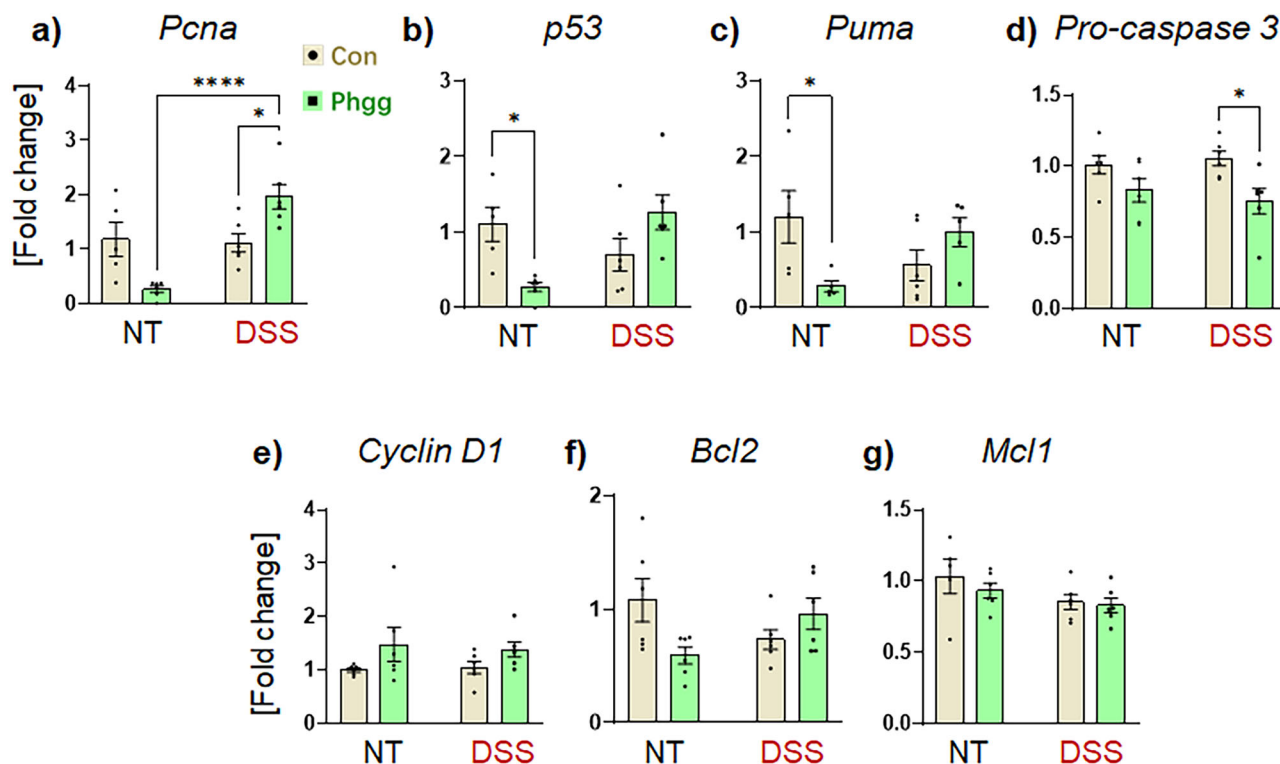
Fig. 4 | Phgg feeding alters colonic expression of genes related to proliferation and apoptosis. Colonic mRNA levels of **a** *Proliferating cell nuclear antigen (Pcna)*, (**b**) *Gene encoding protein p53*, (**c**) *p53 upregulated modulator of apoptosis (Puma)*, (**d**) *Pro-caspase3*, (**e**) *Cyclin D1*, (**f**) *B-cell lymphoma 2 (Bcl2)*, and **g** *Myeloid cell leukemia 1 (Mcl1)*. Values are presented as mean ± SEM. *$p < 0.05$, ***$p < 0.001$, and ****$p < 0.0001$.

levels of genes regulating cell proliferation and apoptosis in both the control and Phgg-fed groups. Since the proximal colon region in the AOM/DSS model did not exhibit tumorigenesis, we selected this region to represent the non-tumor-bearing area. The distal colon region displayed extensive tumorigenesis, especially in the Phgg-fed group, therefore, we selected distal colon to represent tumor-prone area. Remarkably, the distal colon displayed increased mRNA transcripts of *Pcna* exclusively in Phgg-fed group (Fig. 5j). Furthermore, colonic expression of *Bcl2*, whose overexpression is known to suppress apoptosis and promote cell survival[48], was significantly elevated in the Phgg-fed group that received AOM/DSS (Fig. 5k). The expression of *Mcl1*, a pro-survival member of the *Bcl2* protein family[49], was also augmented in the proximal region of Phgg-fed group (Fig. 5l). Moreover, both proximal and distal region of Phgg-fed group displayed increased expression of *cyclin D1*, a regulator of cell cycle progression (Fig. 5m). The increased expression of genes suppressing apoptosis, promoting survival, and regulating cell cycle progression in both proximal and distal regions (Fig. 5k–m) suggest that Phgg supplementation may contribute to a pro-tumorigenic environment, leading to extensive tumorigenesis in the AOM/DSS-treated mice.

Gender-based differences in CRC incidence have been observed in humans, with males showing a relatively higher occurrence than females[50]. To assess whether Phgg feeding displays a similar pattern in CAC development, we next investigated colon tumorigenesis in the female cohort under a similar intervention. Similar to male mice, Phgg-fed female mice experienced more body weight loss and developed extensive colon tumors after AOM/DSS treatment (Fig. 6a–e). Remarkably, control diet-fed female mice treated with AOM/DSS did not develop any visible colon tumors. As evidenced by histochemical staining, colon tumors in Phgg-fed female mice invaded the submucosa and exhibited increased nuclear localization of β-catenin and decreased levels of Ki67 expression in the tumor region (Fig. 6f–i). Our comparative analysis of colon tumor area, β-catenin-positive nuclei, and Ki67 levels revealed comparable tumorigenesis in both male and female mice (Fig.6j–l). Taken together, these results suggest that Phgg

supplementation increased susceptibility to colitis and promoted colon tumorigenesis in both male and female mice.

Diet with lower amount of Phgg also aggravates colonic inflammation and carcinogenesis

To investigate whether a reduced intake of Phgg has distinct effects on colitis and CAC development, we formulated a low-Phgg diet (L-Phgg) containing one-third amount of Phgg (2.5% w/w) than the regular Phgg diet used in this study. To maintain equivalent total fiber content (10% w/w), we proportionally increased the cellulose content from 2.5% to 7.5% in the low-phgg diet. Similar to the Phgg study, 4-week-old WT mice were placed on either a control (Con) or low Phgg diet (L-phgg; 2.5% w/w Phgg and 7.5% w/w cellulose) diet for 4 weeks. Then both groups were transitioned to a DSS (1.4%) containing water for 7 days (Fig. 7a). Lower amount of Phgg consumption exacerbated colonic inflammation, as evidenced by a 4% greater loss in body weight compared to the control group, elevated serum Lcn2 and SAA (Fig. 7b–g). The L-Phgg group showed an increasing trend in colonic Lcn2 levels, but did not reach statistical significance ($p = 0.0649$) (Fig. 7h). Histological analysis further supported the increased severity of colonic inflammation, showing more disrupted crypt structure and reduced level of mucin in the L-Phgg group than control (Fig. 7i).

To elucidate how this lower amount of Phgg impacts colon tumorigenesis, we employed the AOM/DSS model as described previously (Fig. 8a). The L-Phgg group consistently exhibited lower body weight, however, no mortality was observed in this group (Fig. 8b, c). Notably, the L-Phgg group also exhibited colon tumorigenesis, although tumors were not visually apparent to the same extent as in the regular Phgg group (Fig. 8d, e). Histological analysis confirmed the presence of colorectal polyps (Fig. 8f). Indeed, the tumor-occupied colon area in the L-Phgg group was substantially lower (~5% of total colon area) than the Phgg-fed group (~20% of total colon area). Immunohistochemical analysis revealed an increase in β-catenin nuclear localization and a decrease in Ki67 expression in the tumor regions, mirroring the trends observed in the Phgg-fed AOM/DSS
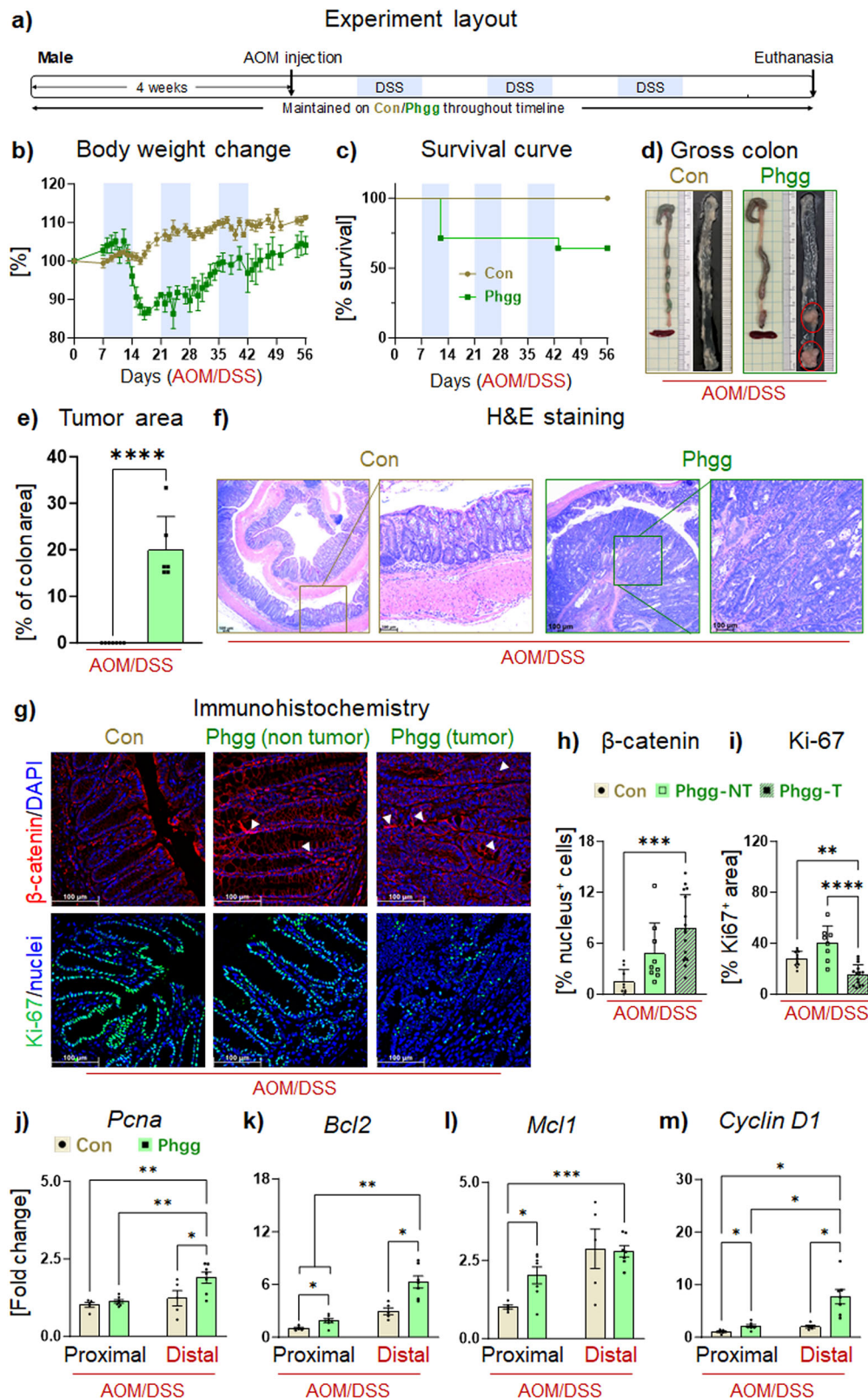
Fig. 5 | Phgg exacerbated colitis-associated colorectal cancer in AOM/DSS male mice. a Experimental timeline, mice were maintained on either Phgg-contained or the control diet. Azoxymethane was administrated (AOM, 7.5 mg/kg body weight, i.p.) 1 week before three 7-day cycles of DSS/regular water (1%, 0.75%, 0.75% of DSS in drinking water), then sacrificed after one more week of regular water. **b** Changes in body weight referred to the weight on the AOM injection day. **c** Probability of survival. **d** Representative pictures of gross colons. **e** Tumor area as percentage of colon area. **f** Representative H&E-stained colon sections (original magnification, ×16, ×100). **g** Representative images of β-catenin (red) and Ki67 (green) immunohistochemical staining. DAPI was used to visualize the nucleus [blue, (original magnification, ×200)]. Quantitative evaluation of **h** β-catenin (nuclear localization) and **i** Ki67 positive cells normalized per unit area. Colonic mRNA levels of **j** *Pcna*, (**k**) *Bcl2*, (**l**) *Mcl1*, and **m** *Cyclin D1*. Values are presented as mean ± SEM. *$p < 0.05$, **$p < 0.01$, ***$p < 0.001$, and ****$p < 0.0001$.
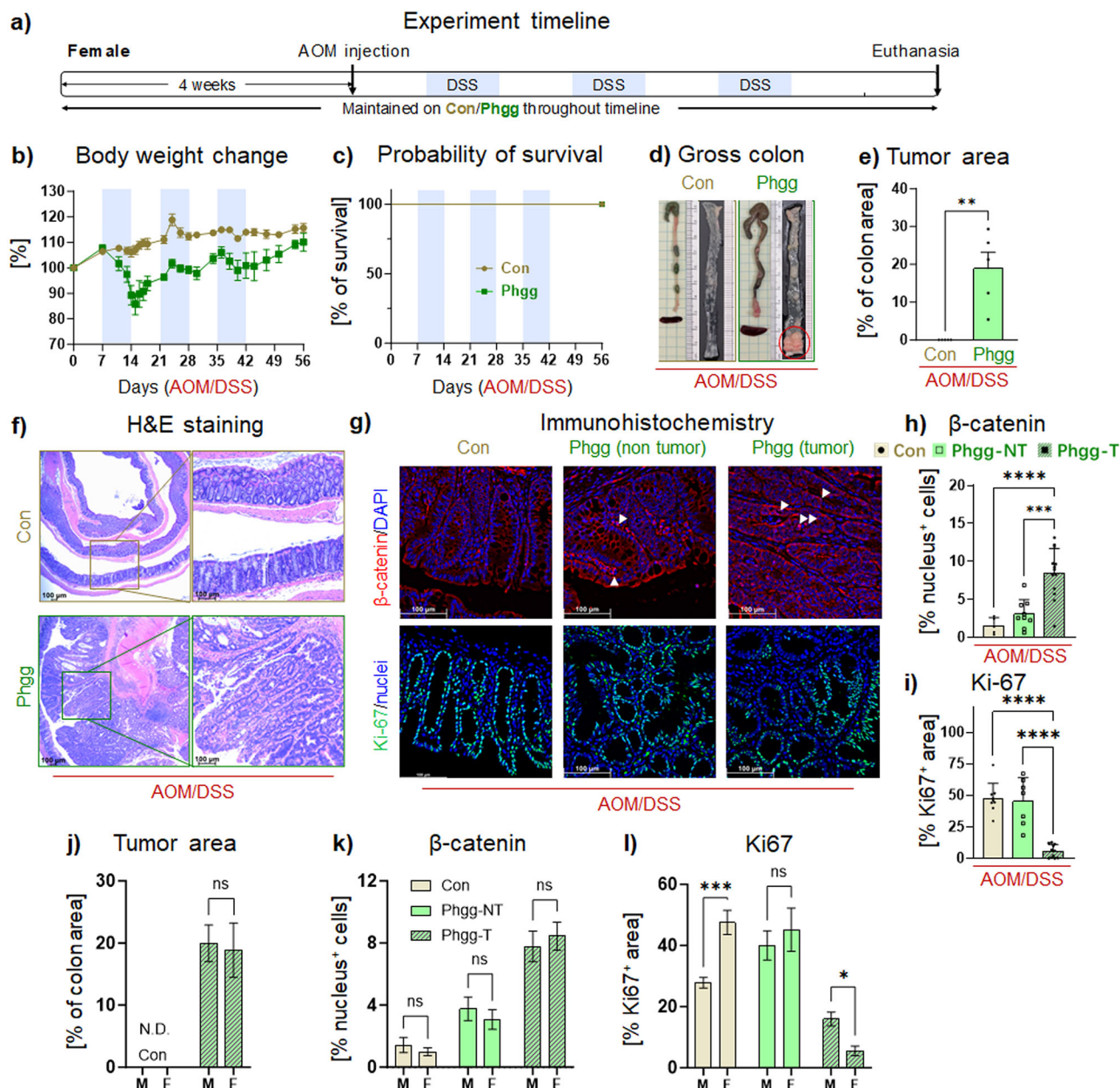
Fig. 6 | Phgg-fed female mice exhibited colon tumorigenesis comparable to that of male mice. a Experimental timeline. **b** Change of body weight referred to the weight on the AOM injection day. **c** Probability of survival. **d** Representative images of the gross colon. **e** Tumor area in percentage of the total colon surface area. **f** Representative images on H&E staining (original magnification, ×16, ×100). **g** Representative images of β-catenin (red) and Ki67 (green) immuno-histochemical staining counterstained with DAPI (blue; original magnification, ×200). Quantitative evaluation of (**h**) β-catenin (nuclear localization) and **i** Ki67 positive cells normalized per unit area. **j–l** Comparative analysis of colon tumor area, β-catenin-positive nuclei, and Ki67 levels between male and female cohort. **j** % tumor area, (**k**) β-catenin (nuclear localization). **l** Ki67 positive cells. Values are presented as mean ± SEM. *$p < 0.05$, **$p < 0.01$, ***$p < 0.001$, and ****$p < 0.0001$.

cohort (Fig. 8g–i). Most notably, no visible tumor was observed in the control group that received AOM/DSS (Fig. 8).

Discussion

Emerging studies indicate that the effect of DFs on intestinal health varies depending on the presence or absence of ongoing inflammation. In particular, soluble DFs generally have beneficial effects on gastrointestinal health[51–55] in individuals with a healthy gut. However, these DFs may have adverse effects on clinical outcomes in patients with IBD[20,56,57]. Our study demonstrates that Phgg has no adverse effects in healthy mice without colonic inflammation. However, in the experimental group with ongoing inflammation, Phgg exacerbated colonic inflammation and induced

extensive colon tumorigenesis. Mechanistically, Phgg supplementation induced imbalanced alterations in intestinal immune activity, favoring inflammation by increasing the production of pro-inflammatory chemo-kines and cytokines and by suppressing the release of anti-inflammatory cytokines. Additionally, mice fed a Phgg-supplemented diet exhibited aberrant expression of genes regulating gut barrier function, cell proliferation, apoptosis, and tumor suppression, leading to increased susceptibility to CAC in the AOM/DSS model.

The Dietary Guidelines for Americans 2020–2025 recommend 28–34 g of total fiber intake for men and women, while the average DF intake of Americans is ~15 g per day[7]. DF supplements offer a convenient way to meet the recommended daily intake. As a result, these supplements
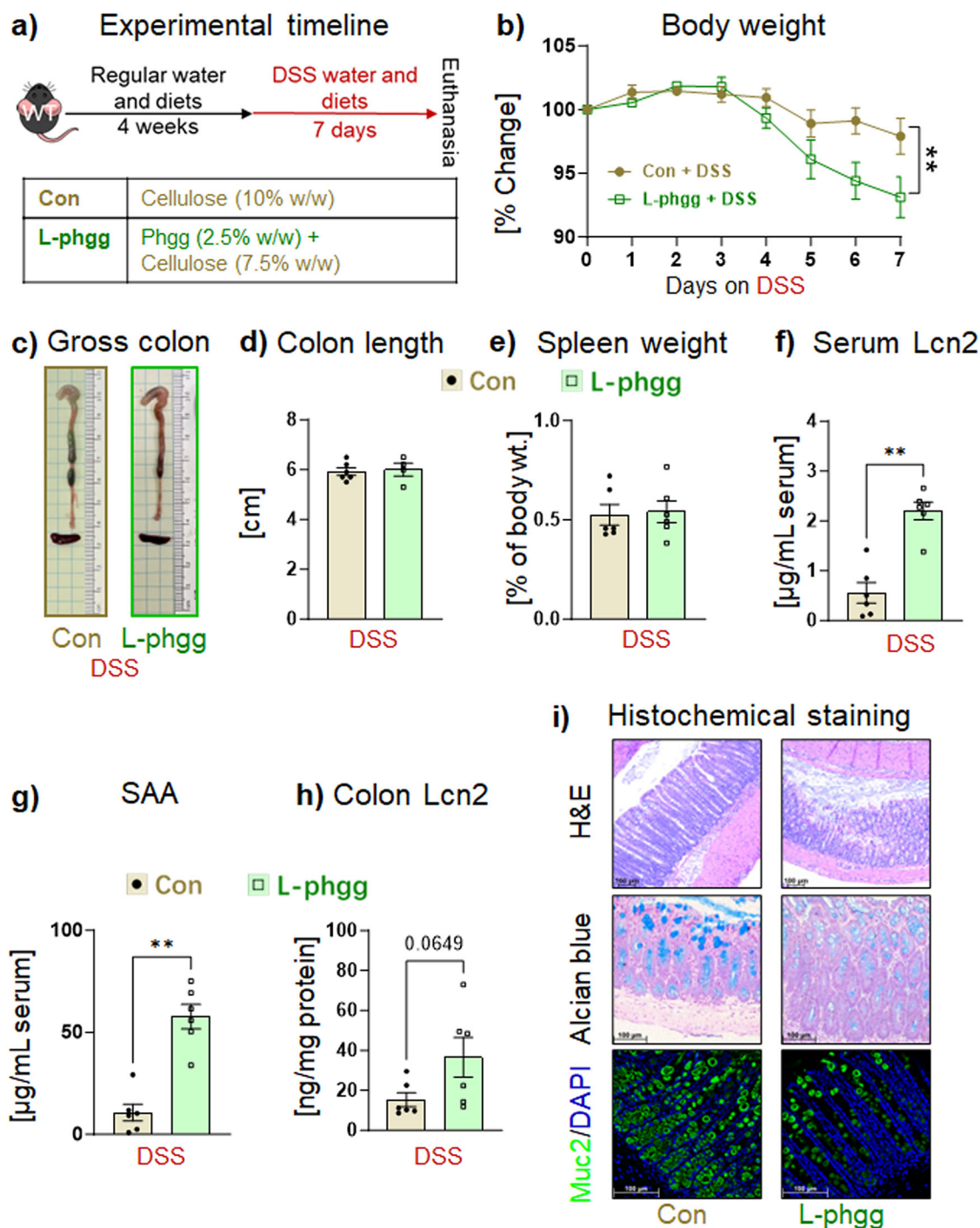
Fig. 7 | Diet with lower Phgg (L-Phgg) also exhibited augmented colitis. a Experiment timeline: 4-week-old WT mice were maintained on either a control (Con) or a Low-Phgg diet for 4 weeks. Afterwards, both groups received 1.4% (w/v) DSS in their drinking water for 7 days. **b** Percent change in body weight. **c** Gross colon appearance. **d** Colon length. **e** Spleen weight as a percent of body weight. Serum levels of **f** SAA and **g** Lcn2. **h** Colonic level Lcn2. **i** Representative images of H&E (original magnification, ×50), Alcian blue (original magnification, ×100), and Muc2 (green, original magnification, ×200) staining. Values are presented as mean ± SEM. $*p < 0.05$, $**p < 0.01$, $***p < 0.001$, and $****p < 0.0001$.

have become a popular choice for bridging nutritional gaps[58]. Unlike natural sources of DF, like fruits and vegetables, which contain a variety of fibers such as cellulose, hemicellulose, pectin, and lignin, DF supplements often consist of a single fiber type. Our understanding of the effects of mono-fiber supplementation on gastrointestinal health, particularly in inflamed intestines, remains limited. The Phgg used in our study is popular as a prebiotic supplement; a detailed evaluation is required to understand specifically how processed forms of Phgg impact intestinal health in individuals with certain

clinical conditions, including IBD. Experimental findings from our mouse model study indicate that Phgg, a prebiotic supplement, may not benefit intestinal health, as it increased susceptibility to colonic inflammation and promoted colon tumorigenesis. To understand the underlying mechanisms, we examined the colonic expression of inflammatory proteins that play a critical role in the progression and development of intestinal inflammation and CAC. CXCL1, a member of the C-X-C chemokine family, induces chemotaxis and infiltration of immune cells, primarily neutrophils, and
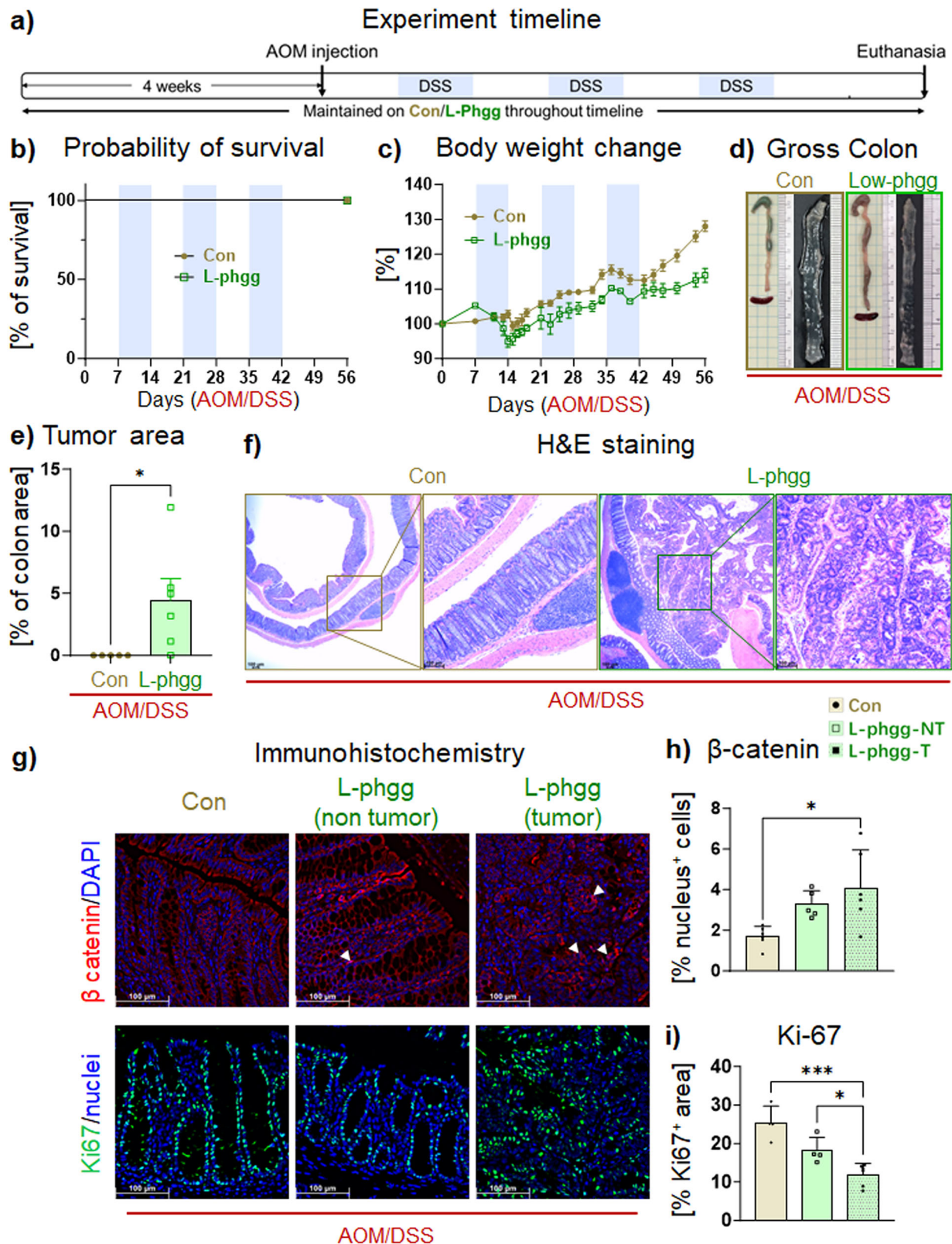
Fig. 8 | Diet containing a low amount of Phgg also promoted colon tumorigenesis. a Experiment timeline. **b** Probability of survival. **c** Percent change in body weight. **d** Representative gross colon images. **e** Tumor-occupied area as a percentage of total colon area. **f** Representative images of H&E-stained colon sections (original magnification, ×16, ×100). **g** Representative images displaying immunohistochemical staining for β-catenin (red, upper panel) and Ki67 (green). DAPI was used to visualize the nucleus [blue, (original magnification, ×200)]. Quantitative evaluation of (**h**) β-catenin (nuclear localization) and **i** Ki67 positive cells normalized per unit area. Values are presented as mean ± SEM. *$p < 0.05$, ***$p < 0.001$.

contributes to the development of colitis[59]. Cxcl1 signals through G protein-coupled chemokine receptor Cxcr2 and is shown to promote tumor growth, proliferation, and metastasis of malignant cells in CRC[60,61]. The Phgg-fed group exhibited elevated colonic levels of Cxcl1, both at the mRNA and protein levels, suggesting its potential role in the Phgg-induced exacerbation of colitis and CAC development. IL-6 and IL-1β, key regulators of chronic intestinal inflammation, play roles in both colitis and colon tumorigenesis[62–65]. IL-6 activates STAT3 to promote tumor initiation and growth[66] and drives Fos-related antigen 1(FOSL1/FRA1) deacetylation, endowing CRC cells with stem cell-like properties and enhancing their proliferation[67]. The inflammatory cytokine IL-1β has also been shown to mediate colonic inflammation[64] and facilitate the stemness and invasiveness of CRC cells through the epithelial-mesenchymal transition activator zinc finger E-box binding homeobox 1[65]. In our study, elevated levels of these inflammatory cytokines were observed along with Cxcl1 in mice fed Phgg, suggesting a collective role of chemokines and cytokines in the Phgg-mediated exacerbation of intestinal inflammation and colon carcinogenesis. Inflammatory cytokines, including IL-6 and IL-1β, increase intestinal permeability[68–70]. In agreement, we observed aberrant expression of TJ proteins in Phgg-fed groups that received DSS. Similar to what was observed in human colon carcinoma tissues[71,72], we found increased colonic mRNA levels of claudin-1 and -2, and decreased claudin-7, in the Phgg-fed group. Increased expression of claudin-1 and -2, coupled with reduced claudin-7, has been observed in IBD[39]. Additionally, elevated colonic levels of both claudin-1 and -2 are known to be linked to increased colon tumorigenesis in humans[73–76]. Interestingly, colonic *Il10* mRNA level was elevated in the control group, but not in the Phgg-fed group, and may have contributed to limiting inflammation in the control diet-fed group following DSS intervention.

PCNA is a crucial protein for the development of CRC by participating in DNA replication and repair, which are essential for tumor growth and progression. PCNA acts as a sliding clamp for DNA polymerase during the synthesis of new DNA strands, ensuring accurate replication during the S phase of the cell cycle. In CRC, PCNA is often overexpressed, and this heightened expression correlates with increased cellular proliferation and more aggressive cancer characteristics[77]. Additionally, PCNA is closely associated with Cyclin D1, a regulator of the G1-to-S phase transition in the cell cycle, as both proteins are involved in regulating the cell cycle and ensuring efficient DNA replication during tumor growth[78,79]. Notably, the Phgg+DSS groups showed elevated mRNA expression of both *Pcna* and *Cyclin D1*, indicating that Phgg-induced changes in cell proliferation regulators potentiating CRC development in the AOM/DSS group. Moreover, *Mcl1* (myeloid cell leukemia 1) is a widely recognized pro-survival member of the *Bcl2* (B-cell lymphoma protein 2) and is notably recognized for its anti-apoptotic role in the Bcl2 family[49]. The colonic expression of both *Mcl1* and *Bcl2* was increased in the Phgg-fed group that received AOM/DSS. Collectively, the increased expression of genes regulating proliferation and pro-survival specifically in the proximal region indicates that Phgg supplementation promoting a pro-tumorigenic environment, leading to extensive tumorigenesis in the AOM/DSS-treated mice. The colonic tumors observed in the Phgg-fed group displayed a significant increase in nuclear translocation of β-catenin, indicating an activation of the Wnt-β-catenin signaling pathway. Interestingly, a moderate increase in β-catenin nuclear localization was also observed in the adjacent non-tumor regions of the Phgg-fed groups compared to the control, implying a possible predisposition to tumorigenesis. Observations from human CRC cohorts report variable findings regarding Ki67, a cell proliferation marker, expression and its association with overall survival in CRC patients. For example, higher Ki67 expression in colon tumor regions has been linked to improved clinical outcomes[80], particularly in CRC patients receiving adjuvant chemotherapy[81]. Notably, increased proliferation activity in rectal cancer patients has also been associated with improved survival[47]. Conversely, other studies suggest that higher Ki67 expression indicates lower survival rates[82,83] and poor prognosis[84]. We observed reduced Ki67 expression in the tumor regions compared to adjacent normal tissues. A longer-term study will help investigate whether reduced Ki67 expression in the Phgg-fed group is linked to increased colon tumor burden and the development of advanced colorectal neoplasms. Our findings from colon gene expression analysis indicate that Phgg-induced alterations in immune activity, barrier function, and cell survival markers predisposed mice to colitis and CRC development. This conjecture requires further confirmation using in vitro models, such as colonic organoid co-culture systems, to better understand how interactions between Phgg-mediated microbial metabolites and intestinal epithelial or immune cells influence inflammatory signaling, barrier integrity, and cell viability.

In summary, our findings suggest potential risks associated with isolated Phgg consumption, particularly as a supplement for individuals with ongoing intestinal inflammation. The amount of Phgg fiber used in this preclinical study would be difficult to achieve through everyday food intake in humans. However, given the popularity of prebiotic supplements and prebiotic fiber-containing processed food products, human consumption of these fibers could constitute a significant portion of daily intake. Upcoming preclinical studies should focus on assessing the dose-dependent effects of processed Phgg on intestinal health and gut microbiome, a recognized modulator of both IBD and CRC, in the long run, both in the presence and absence of inflammation. A detailed understanding of the intricate interplay between continuous exposure to single DF and the host microbiome and intestinal health, particularly in the context of IBD, is essential. This experimental knowledge is vital for developing personalized nutrition strategies that account for individual health conditions to optimize DF intake and minimize potential adverse consequences.

Methods

Mice and diets
C57BL/6 wild-type (WT) mice were bred and maintained under specific pathogen-free conditions in a humidity- and temperature-controlled room at The Pennsylvania State University in University Park, Pennsylvania. At 4 weeks of age, mice were divided into experimental groups. Throughout the study, mice had unrestricted access to experimental diets (control, Phgg-containing diet, or low-Phgg diet) and water. The diets were prepared by Research Diets, Inc. (New Brunswick, NJ). A detailed composition of all three diets is provided in Table 1. Food, water, and cages were replaced weekly. All experimental procedures were conducted in compliance with the ethical guidelines and standards approved by the Institutional Animal Care and Use Committee at The Pennsylvania State University.

DSS-induced colitis study
Four-week-old C57BL/6 wild-type mice were fed control or Phgg-containing diets for 4 weeks. These mice were then randomly divided into two groups: a basal-feeding group (NT) and a colitis group. Colitis was induced by administering drinking water containing 1.4% w/v dextran sulfate sodium (DSS, MP Biomedicals) for 7 days. Daily body weights were monitored throughout the DSS period. The NT groups receiving control or the Phgg diet were maintained on water only.

Colitis-associated colorectal cancer study
Four-week-old WT mice were fed with either control or Phgg diet. After 4 weeks of diet feeding, both control and Phgg diet received a single dose of azoxymethane (AOM, 7.5 mg/kg, i.p.). One week later, DSS/regular water cycles began, starting with 1.0% DSS water and then decreasing to 0.75% for the remaining two cycles. Each cycle consisted of 14 days, with 7 days of DSS water followed by 7 days of regular water. The mice were euthanized 1 week after completing the final cycle. All mice continued their assigned diets throughout the experiment and were monitored for their body weights regularly.

Sample collection and preparation
Upon completion, mice were humanely euthanized using CO_2. Blood was collected into serum-separation tubes, followed by centrifugation at $8000 \times g$ for 8 min at room temperature. The serum was then stored at

Table 1 | Diet composition

Diet component	Cellulose-containing diet (Con)		Partially hydrolyzed guar gum (Phgg) diet		Low-Phgg (L-Phgg) diet	
Product #	D12081402		D22030208		D23033103	
	gm%	kcal%	gm%	kcal%	gm%	kcal%
Protein	18.5	20	19	20	18.6	20
Carbohydrate	61.8	65	63.4	65	62.3	65
Fat	6.4	15	6.5	15	6.4	15
Total		100		100		100
Kcal/gm		3.78		3.88		3.82
Ingredients	g	kcal	g	kcal	g	kcal
Casein, 30 Mesh	200	800	200	800	200	800
L-cysteine	3	12	3	12	3	12
Corn starch	409	1636	381	1524	400	1600
Maltodextrin 10	110	440	110	440	110	440
Dextrose	150	600	150	600	150	600
Cellulose, BW200	100	0	25	0	75	0
Partially hydrolyzed guar gum (Phgg)	0	0	75	112.5	25	37.5
Soybean oil	70	630	70	630	70	630
Mineral mix S10026	10	0	10	0	10	0
Dicalcium PO$_4$	13	0	13	0	13	0
Calcium carbonate	5.5	0	5.5	0	5.5	0
Potassium citrate	16.5	0	16.5	0	16.5	0
Vitamin mix V10001	10	40	10	40	10	40
Choline bitartrate	2	0	2	0	2	0
Yellow Dye #5, FD&C	0	0	0.025	0	0	0
Red Dye #40, FD&C	0	0	0	0	0.05	0
Blue Dye #1, FD&C	0.05	0	0.025	0	0	0
Total	1099.05	4158	1071.05	4159	1090.05	4160

−80 °C until analysis. Colon segments were snap-frozen in liquid nitrogen, collected in RNAlater solution, or fixed in 10% neutral buffered formalin (NBF) for cytokine/chemokine measurement via ELISA, mRNA expression via qPCR, and histochemical staining, respectively.

Colon protein extraction and quantification
The colon segments were homogenized in RIPA buffer (Thermo Scientific™, FNN0021) containing protease inhibitor (Thermo Scientific™, 78429) and phosphatase inhibitors (Thermo Scientific™, 78428), followed by centrifugation at $12,000 \times g$ at 4 °C for 5 min. The supernatants were then collected, and the total protein concentration was determined using a Pierce™ bicinchoninic acid protein assay kit (Thermo Scientific™, 23225) according to the manufacturer's instructions.

Enzyme-linked immunosorbent assay
Using enzyme-linked immunosorbent assay (ELISA) kits from R&D Systems, SAA (DY2948) and lipocalin 2 (Lcn2, DY1857) were measured in serum. Similarly, the levels of Lcn2, interleukin-1β (IL-1β, DY401), IL-1 receptor antagonist (IL1Ra, DY480), IL-6 (DY406), and C-X-C motif chemokine ligand 1 (CXCL-1, DY453) were determined

in colon protein extracts. All analyses were conducted following the manufacturer's recommended protocols, with prior titration and appropriate dilutions.

RNA isolation and quantitative polymerase chain reaction (qPCR)
The colon tissues were homogenized, and total RNA was extracted using TRIZOL reagent (Invitrogen) following the manufacturer's instructions. The concentration of the extracted RNA was estimated with a NanoDrop spectrophotometer (Thermo Scientific). The RNA obtained from DSS-treated groups was purified via the lithium chloride precipitation method. RNA was then converted to complementary DNA with the ScriptTM XLT cDNA supermix kit (QuantaBio) according to the manufacturer's instructions. qPCR was performed to assess the expression of colonic genes encoding inflammatory, proliferative, apoptotic, and TJ markers using SYBR Green master mix (Thermo Fisher) on QuantStudio 3 Real-Time PCR System (Applied Biosystems). Relative expression levels were calculated by $2^{-\Delta\Delta Ct}$, with 36B4 and β-actin as an endogenous reference for normalization. A list of the primers is provided in Table 2.

Histochemical analysis
For histochemical staining, colon tissue was dissected from the mice, and feces were flushed with ice-cold PBS to clean the colon, and a Swiss roll was prepared and fixed in 10% NBF for 24 h. After that, the Swiss roll tissue was transferred to 70% ethanol. Further, the colon was dehydrated using an alcohol gradient (70%, 90%, 95%, and 100%), followed by two treatments with xylene. The tissue was then embedded in paraffin wax and sectioned (thickness 5 μM) using a microtome. The paraffin-embedded tissue sections were deparaffinized in xylene and rehydrated with a gradient of alcohol (100%, 95%, 70%, and 50%) using a Leica Autostainer XL (Leica Biosystems).

Hematoxylin and Eosin (H&E) staining was performed by the Animal Diagnostic Laboratory, The Pennsylvania State University, and imaged by a Leica DMi8 microscope, Leica Microsystems. For alcian blue staining, the colon sections were deparaffinized using a Leica Autostainer XL (Leica Biosystems) and then stained with Alcian blue (Vector Laboratories Inc.) following the manufacturer's instructions to evaluate goblet cell-containing acidic mucus.

Immunofluorescence staining
Immunohistochemical staining was performed as described in our previous studies[21,23]. Briefly, deparaffinized sections were incubated in pre-warmed sodium citrate buffer (pH 6.0) at 98 °C for 20 min in a water bath, followed by washing with PBS. To block the non-specific sites, the tissue sections were then incubated with 10% donkey serum containing 0.3% Triton X-100 (VWR Life Sciences) for 90 min at room temperature. Subsequently, the sections were incubated overnight at 4 °C with primary antibodies [β-catenin (Novus Biologicals); Ki67 (Novus Biologicals); Muc2 (Abcam), or Lcn2 (R&D Systems)] diluted in PBS containing 1% donkey serum (Sigma-Aldrich), 1% bovine serum albumin (BSA, Sigma-Aldrich), and 0.3% Triton X-100. After incubation, the sections were washed with PBS three times and then incubated with the secondary antibody [anti-mouse Alexa Fluor™ 555 (β-catenin), anti-rabbit Alexa Fluor™ 488 (Ki67), or anti-goat Alexa Fluor™488] for 90 min at room temperature in a dark chamber, followed by mounting with antifade reagent containing 4′,6′-diamidino-2-phenylindole and an anti-fading agent (Sigma Fluoroshield™, F6057) for nucleus staining. All histological images were captured using the Leica DMi8 with the LAS X software (Leica Microsystems Inc.) and quantified using ImageJ software.

Image quantification
The colon tumor area, Ki67 expression, and β-catenin localization were quantified using ImageJ software with the Fiji extension. The entire colon area and the tumor area were automatically identified through color-

Table 2 | List of primers

Target genes	Forward (5′-3′)	Reverse (5′-3′)	Reference
36B4	TCC AGG CTT TGG GCA TCA	CTT TAT TCA GCT GCA CAT CAC TCA GA	85
β-actin	GCC AAC CGT GAA AAG ATG ACC	GAG GCA TAC AGG GAC AGC AC	86
Bcl2	AGC CTG AGA GCA ACC CAA T	AGC GAC GAG AGA AGT CAT CC	87
Pro-caspase3	ACA TGG GAG CAA GTC AGT GG	CGT CCA CAT CCG TAC CAG AG	87
Cldn1	AGC ACC GGG CAG ATA CAG T	ATG CCA ATT ACC ATC AAG GC	88
Cldn2	GTC ATC GCC CAT CAG AAG AT	ACT GTT GGA CAG GGA ACC A	89
Cldn4	CGT AGC AAC GAC AAG CCC TA	TGT CCC CAG CAA GCA GTT AG	90
Cldn5	GTT AAG GCA CGG GTA GCA CT	TAC TTC TGT GAC ACC GGC AC	90
Cldn7	AGG GTC TGC TCT GGT CCT T	GTA CGC AGC TTT GCT TTC A	91
Cldn10	CCC AGA ATG GGC TAC ACA TA	CCT TCT CCG CCT TGA TAC TT	90
Cxcl1	AGC TGC GCT GTC AGT GCC	CAA GCC TCG CGA CCA TTC	60
Cyclin D1	GCG TAC CCT GAC ACC AAT CT	ATC TCC TTC TGC ACG CAC TT	92
E-cadherin	ACT TGG GGA CAG CAA CAT CA	GGG TTT AAA TCG GCC AGC A	93
IL-4	TCG GCA TTT TGA ACG AGG TC	GAA AAG CCC GAA AGA GTC TC	94
IL-6	CCA CTT CAC AAG TCG GAG GCT TA	GCA AGT GCA TCA TCG TTG TTC ATA C	95
IL-10	ACC TGC TCC ACT GCC TTG CT	GGT TGC CAA GCC TTA TCG GA	96
Stat3	AGC TGG ACA CAC GCT ACC T	AGG AAT CGG CTA TAT TGC TGG T	97
iNos	CTT TGC CAC GGA CGA GAC	TCA TTG TAC TCT GAG GGC TGA C	98
Mcl1	AAA GGC GGC TGC ATA AGT C	TGG CGG TAT AGG TCG TCC TC	99
Mcp1	ATC CCA ATG AGT AGG CTG GAG AGC	CAG AAG TGC TTG AGG TGG TTG TG	100
p53	CTC CGA AGA CTG GAT GAC TGC	CAA CAG ATC GTC CAT GCA GTG	101
Pcna	CAA GTG GAG AGC TTG GCA ATG G	GCA AAC GTT AGG TGA ACA GGC TC	102
Puma	ACG ACC TCA ACG CAC AGT ACG	TCC CAT GAT GAG ATT GTA CAG GAC	103
Tnfα	ACT CCA GGC GGT GCC TAT GT	AGT GTG AGG GTC TGG GCC AT	104
Zo1	ACC CGA AAC TGA TGC TGT GGA TAG	AAA TGG CCG GGC AGA ACT TGT GTA	89
Zo2	AGC TTG TAG TTC TGA GCC GC	CCG ACA CGG CAA TTC CAA AT	90
Zo3	GGC TGA TTG TTT CCA GGC CC	CCA GAG ACA GCT ATG CCG AA	90

based selection. Ki67 expression was estimated by the stained area in the green channel (Ki67) normalized by the stained area in the blue channel (nucleus). The nuclear localization of β-catenin was identified by counting the number of overlapping areas between the red channel (β-catenin) and the blue channel (nucleus) after filtering with watershed. The number of nuclei was counted by the number of areas with a circularity greater than 90% for an ellipse after filtering with watershed in the blue channel. Both numbers were counted using the particle measure function. The number of β-catenin-positive nuclei was then normalized by the total number of nuclei.

Statistical analysis

All data are presented as mean ± SEM. The assessment of normality and equal variance was conducted using the Shapiro–Wilk and Bartlett tests within RStudio. Statistical significance between the two groups was determined via an unpaired, two-tailed t-test (parametric) or an unpaired non-parametric Mann–Whitney test. The threshold for statistical significance was set at $p < 0.05$. Comparisons involving more than two groups, one-way ANOVA or Welch and Brown-Forsyth ANOVA were applied for parametric and non-parametric data, respectively, followed by Tukey's multiple comparison tests. The differences were considered significant with a p value less than 0.05 and are represented as $*p < 0.05$, $**p < 0.01$, $***p < 0.001$, and $****p < 0.0001$.

Data availability

The original data generated in this study is included in this article. Further inquiries can be directed to the corresponding author.

References

1. Sung, H. et al. Global cancer statistics 2020: GLOBOCAN estimates of incidence and mortality worldwide for 36 cancers in 185 countries. *CA Cancer J. Clin.* **71**, 209–249 (2021).
2. Bray, F. et al. Global cancer statistics 2022: GLOBOCAN estimates of incidence and mortality worldwide for 36 cancers in 185 countries. *CA Cancer J. Clin.* **74**, 229–263 (2024).
3. Bujanda, L., Cosme, A., Gil, I. & Arenas-Mirave, J. I. Malignant colorectal polyps. *World J. Gastroenterol.* **16**, 3103–3111 (2010).
4. Amersi, F., Agustin, M. & Ko, C. Y. Colorectal cancer: epidemiology, risk factors, and health services. *Clin. Colon Rectal Surg.* **18**, 133–140 (2005).
5. Johnson, C. M. et al. Meta-analyses of colorectal cancer risk factors. *Cancer Causes Control* **24**, 1207–1222 (2013).
6. von Roon, A. C. et al. The risk of cancer in patients with Crohn's disease. *Dis. Colon Rectum* **50**, 839–855 (2007).
7. Reynolds, A. et al. Carbohydrate quality and human health: a series of systematic reviews and meta-analyses. *Lancet* **393**, 434–445 (2019).
8. Lee, S. H., Moore, L. V., Park, S., Harris, D. M. & Blanck, H. M. Adults meeting fruit and vegetable intake recommendations—United States, 2019. *MMWR Morb. Mortal. Wkly Rep.* **71**, 1–9 (2022).
9. Chau, C. F. & Huang, Y. L. Effects of the insoluble fiber derived from Passiflora edulis seed on plasma and hepatic lipids and fecal output. *Mol. Nutr. Food Res.* **49**, 786–790 (2005).

10. Gill, S. K., Rossi, M., Bajka, B. & Whelan, K. Dietary fibre in gastrointestinal health and disease. *Nat. Rev. Gastroenterol. Hepatol.* **18**, 101–116 (2021).

11. Hunt, J. E., Hartmann, B., Schoonjans, K., Holst, J. J. & Kissow, H. Dietary Fiber Is Essential to Maintain Intestinal Size, L-Cell Secretion, and Intestinal Integrity in Mice. *Front. Endocrinol.* **12**, 640602 (2021).

12. Macia, L. et al. Metabolite-sensing receptors GPR43 and GPR109A facilitate dietary fibre-induced gut homeostasis through regulation of the inflammasome. *Nat. Commun.* **6**, 6734 (2015).

13. Boffa, L. C. et al. Modulation of colonic epithelial cell proliferation, histone acetylation, and luminal short chain fatty acids by variation of dietary fiber (wheat bran) in rats. *Cancer Res.* **52**, 5906–5912 (1992).

14. Goodlad, R. A., Ratcliffe, B., Fordham, J. P. & Wright, N. A. Does dietary fibre stimulate intestinal epithelial cell proliferation in germ free rats?. *Gut* **30**, 820–825 (1989).

15. Zhang, J. & Lupton, J. R. Dietary fibers stimulate colonic cell proliferation by different mechanisms at different sites. *Nutr. Cancer* **22**, 267–276 (1994).

16. Abe, A. et al. Partially hydrolyzed guar gum is associated with improvement in gut health, sleep, and motivation among healthy subjects. *J. Clin. Biochem. Nutr.* **72**, 189–197 (2023).

17. Hiel, S. et al. Effects of a diet based on inulin-rich vegetables on gut health and nutritional behavior in healthy humans. *Am. J. Clin. Nutr.* **109**, 1683–1695 (2019).

18. Valcheva, R. et al. Inulin-type fructans improve active ulcerative colitis associated with microbiota changes and increased short-chain fatty acids levels. *Gut Microbes* **10**, 334–357 (2019).

19. Bretin, A. et al. Psyllium fiber protects against colitis via activation of bile acid sensor farnesoid X receptor. *Cell Mol. Gastroenterol. Hepatol.* **15**, 1421–1442 (2023).

20. Armstrong, H. K. et al. Unfermented beta-fructan fibers fuel inflammation in select inflammatory bowel disease patients. *Gastroenterology* **164**, 228–240 (2023).

21. Tian, S. et al. Refined fiber inulin promotes inflammation-associated colon tumorigenesis by modulating microbial succinate production. *Cancer Rep.* **6**, e1863 (2023).

22. Yang, J. et al. High soluble fiber promotes colorectal tumorigenesis through modulating gut microbiota and metabolites in mice. *Gastroenterology* **166**, 323–337 e327 (2024).

23. Paudel, D. et al. Dietary fiber guar gum-induced shift in gut microbiota metabolism and intestinal immune activity enhances susceptibility to colonic inflammation. *Gut Microbes* **16**, 2341457 (2024).

24. Miles, J. P. et al. Supplementation of low- and high-fat diets with fermentable fiber exacerbates severity of DSS-induced acute colitis. *Inflamm. Bowel Dis.* **23**, 1133–1143 (2017).

25. Yoon, S. J., Chu, D. C. & Raj Juneja, L. Chemical and physical properties, safety and application of partially hydrolized guar gum as dietary fiber. *J. Clin. Biochem Nutr.* **42**, 1–7 (2008).

26. Parang, B., Barrett, C. W. & Williams, C. S. AOM/DSS model of colitis-associated cancer. *Methods Mol. Biol.* **1422**, 297–307 (2016).

27. Waldner, M. J. & Neurath, M. F. Master regulator of intestinal disease: IL-6 in chronic inflammation and cancer development. *Semin. Immunol.* **26**, 75–79 (2014).

28. Lim, A. I. et al. Prenatal maternal infection promotes tissue-specific immunity and inflammation in offspring. *Science* **373**, eabf3002 (2021).

29. Grivennikov, S. et al. IL-6 and Stat3 are required for survival of intestinal epithelial cells and development of colitis-associated cancer. *Cancer Cell* **15**, 103–113 (2009).

30. Paradis, T., Begue, H., Basmaciyan, L., Dalle, F. & Bon, F. Tight junctions as a key for pathogens invasion in intestinal epithelial cells. *Int. J. Mol. Sci.* **22**, 2506 (2021).

31. Tan, Y., Guan, Y., Sun, Y. & Zheng, C. Correlation of intestinal mucosal healing and tight junction protein expression in ulcerative colitis patients. *Am. J. Med. Sci.* **357**, 195–204 (2019).

32. Poritz, L. S. et al. Loss of the tight junction protein ZO-1 in dextran sulfate sodium induced colitis. *J. Surg. Res.* **140**, 12–19 (2007).

33. Poritz, L. S., Harris, L. R. 3rd, Kelly, A. A. & Koltun, W. A. Increase in the tight junction protein claudin-1 in intestinal inflammation. *Dig. Dis. Sci.* **56**, 2802–2809 (2011).

34. Ding, Y. et al. Intestinal Claudin-7 deficiency impacts the intestinal microbiota in mice with colitis. *BMC Gastroenterol.* **22**, 24 (2022).

35. Tanaka, H. et al. Intestinal deletion of Claudin-7 enhances paracellular organic solute flux and initiates colonic inflammation in mice. *Gut* **64**, 1529–1538 (2015).

36. Wang, K. et al. Cldn-7 deficiency promotes experimental colitis and associated carcinogenesis by regulating intestinal epithelial integrity. *Oncoimmunology* **10**, 1923910 (2021).

37. Amasheh, S. et al. Claudin-2 expression induces cation-selective channels in tight junctions of epithelial cells. *J. Cell Sci.* **115**, 4969–4976 (2002).

38. Heller, F. et al. Interleukin-13 is the key effector Th2 cytokine in ulcerative colitis that affects epithelial tight junctions, apoptosis, and cell restitution. *Gastroenterology* **129**, 550–564 (2005).

39. Garcia-Hernandez, V., Quiros, M. & Nusrat, A. Intestinal epithelial claudins: expression and regulation in homeostasis and inflammation. *Ann. N. Y. Acad. Sci.* **1397**, 66–79 (2017).

40. van Roy, F. & Berx, G. The cell-cell adhesion molecule E-cadherin. *Cell Mol. Life Sci.* **65**, 3756–3788 (2008).

41. Umeda, K. et al. ZO-1 and ZO-2 independently determine where claudins are polymerized in tight-junction strand formation. *Cell* **126**, 741–754 (2006).

42. Zhou, H. et al. The prognostic value of proliferating cell nuclear antigen expression in colorectal cancer: a meta-analysis. *Medicine* **97**, e13752 (2018).

43. Fleming, M., Ravula, S., Tatishchev, S. F. & Wang, H. L. Colorectal carcinoma: pathologic aspects. *J. Gastrointest. Oncol.* **3**, 153–173 (2012).

44. Sebio, A., Kahn, M. & Lenz, H. J. The potential of targeting Wnt/beta-catenin in colon cancer. *Expert Opin. Ther. Targets* **18**, 611–615 (2014).

45. Gerdes, J. et al. Cell cycle analysis of a cell proliferation-associated human nuclear antigen defined by the monoclonal antibody Ki-67. *J. Immunol.* **133**, 1710–1715 (1984).

46. Kubota, Y. et al. Ki-67-determined growth fraction versus standard staging and grading parameters in colorectal carcinoma. A multivariate analysis. *Cancer* **70**, 2602–2609 (1992).

47. Salminen, E., Palmu, S., Vahlberg, T., Roberts, P. J. & Soderstrom, K. O. Increased proliferation activity measured by immunoreactive Ki67 is associated with survival improvement in rectal/recto sigmoid cancer. *World J. Gastroenterol.* **11**, 3245–3249 (2005).

48. Yang, J. et al. Prevention of apoptosis by Bcl-2: release of cytochrome c from mitochondria blocked. *Science* **275**, 1129–1132 (1997).

49. Widden, H. & Placzek, W. J. The multiple mechanisms of MCL1 in the regulation of cell fate. *Commun. Biol.* **4**, 1029 (2021).

50. Abancens, M., Bustos, V., Harvey, H., McBryan, J. & Harvey, B. J. Sexual dimorphism in colon cancer. *Front Oncol.* **10**, 607909 (2020).

51. Drabinska, N., Krupa-Kozak, U. & Jarocka-Cyrta, E. Intestinal permeability in children with celiac disease after the administration of oligofructose-enriched inulin into a gluten-free diet-results of a randomized, placebo-controlled, pilot trial. *Nutrients* **12**, 1736 (2020).

52. Polymeros, D. et al. Partially hydrolyzed guar gum accelerates colonic transit time and improves symptoms in adults with chronic constipation. *Dig. Dis. Sci.* **59**, 2207–2214 (2014).

53. Takahashi, H. et al. Influence of partially hydrolyzed guar gum on constipation in women. *J. Nutr. Sci. Vitaminol.* **40**, 251–259 (1994).

54. Chan, T. C. et al. Effectiveness of partially hydrolyzed guar gum in reducing constipation in long term care facility residents: a randomized single-blinded placebo-controlled trial. *J. Nutr. Health Aging* **26**, 247–251 (2022).

55. Russo, F. et al. Inulin-enriched pasta improves intestinal permeability and modifies the circulating levels of zonulin and glucagon-like peptide 2 in healthy young volunteers. *Nutr. Res.* **32**, 940–946 (2012).

56. Gearry, R. B. et al. Reduction of dietary poorly absorbed short-chain carbohydrates (FODMAPs) improves abdominal symptoms in patients with inflammatory bowel disease—a pilot study. *J. Crohns Colitis* **3**, 8–14 (2009).

57. Arifuzzaman, M. et al. Dietary fiber is a critical determinant of pathologic ILC2 responses and intestinal inflammation. *J. Exp. Med.* **221**, e20232148 (2024).

58. Lambeau, K. V. & McRorie, J. W. Jr Fiber supplements and clinically proven health benefits: How to recognize and recommend an effective fiber therapy. *J. Am. Assoc. Nurse Pr.* **29**, 216–223 (2017).

59. Zhao, H. et al. C-X-C Motif Chemokine Ligand 1 Promotes Colitis by Modulating the Gut Microbiota. *J. Innate Immun.* **16**, 33–44 (2024).

60. Zhuo, C., Ruan, Q., Zhao, X., Shen, Y. & Lin, R. CXCL1 promotes colon cancer progression through activation of NF-kappaB/P300 signaling pathway. *Biol. Direct* **17**, 34 (2022).

61. Lukaszewicz-Zajac, M., Paczek, S., Mroczko, P. & Kulczynska-Przybik, A. The significance of CXCL1 and CXCL8 as well as their specific receptors in colorectal cancer. *Cancer Manag Res.* **12**, 8435–8443 (2020).

62. Yang, H. et al. Involvement of NF-kappaB/IL-6 pathway in the processing of colorectal carcinogenesis in colitis mice. *Int. J. Inflam.* **2014**, 130981 (2014).

63. Shahini, A. & Shahini, A. Role of interleukin-6-mediated inflammation in the pathogenesis of inflammatory bowel disease: focus on the available therapeutic approaches and gut microbiome. *J. Cell Commun. Signal.* **17**, 55–74 (2023).

64. Coccia, M. et al. IL-1beta mediates chronic intestinal inflammation by promoting the accumulation of IL-17A secreting innate lymphoid cells and CD4(+) Th17 cells. *J. Exp. Med.* **209**, 1595–1609 (2012).

65. Li, Y., Wang, L., Pappan, L., Galliher-Beckley, A. & Shi, J. IL-1beta promotes stemness and invasiveness of colon cancer cells through Zeb1 activation. *Mol. Cancer* **11**, 87 (2012).

66. Lin, Y. et al. Progress in Understanding the IL-6/STAT3 pathway in colorectal cancer. *OncoTargets Ther.* **13**, 13023–13032 (2020).

67. Wang, T. et al. The inflammatory cytokine IL-6 induces FRA1 deacetylation promoting colorectal cancer stem-like properties. *Oncogene* **38**, 4932–4947 (2019).

68. Al-Sadi, R. et al. Interleukin-6 modulation of intestinal epithelial tight junction permeability is mediated by JNK pathway activation of claudin-2 gene. *PLoS ONE* **9**, e85345 (2014).

69. Rawat, M. et al. IL1B Increases intestinal tight junction permeability by up-regulation of MIR200C-3p, which degrades occludin mRNA. *Gastroenterology* **159**, 1375–1389 (2020).

70. Meyer, F., Wendling, D., Demougeot, C., Prati, C. & Verhoeven, F. Cytokines and intestinal epithelial permeability: a systematic review. *Autoimmun. Rev.* **22**, 103331 (2023).

71. Kinugasa, T. et al. Selective up-regulation of claudin-1 and claudin-2 in colorectal cancer. *Anticancer Res.* **27**, 3729–3734 (2007).

72. Nakagawa, S. et al. Expression of CLDN1 in colorectal cancer: a novel marker for prognosis. *Int. J. Oncol.* **39**, 791–796 (2011).

73. Dhawan, P. et al. Claudin-1 regulates cellular transformation and metastatic behavior in colon cancer. *J. Clin. Investig.* **115**, 1765–1776 (2005).

74. Paquet-Fifield, S. et al. Tight junction protein claudin-2 promotes self-renewal of human colorectal cancer stem-like cells. *Cancer Res.* **78**, 2925–2938 (2018).

75. Wei, M. et al. Claudin-2 promotes colorectal cancer growth and metastasis by suppressing NDRG1 transcription. *Clin. Transl. Med.* **11**, e667 (2021).

76. Buchert, M. et al. Symplekin promotes tumorigenicity by up-regulating claudin-2 expression. *Proc. Natl. Acad. Sci. USA* **107**, 2628–2633 (2010).

77. Guzińska-Ustymowicz, K., Stepień, E. & Kemona, A. MCM-2, Ki-67 and PCNA protein expressions in pT3G2 colorectal cancer indicated lymph node involvement. *Anticancer Res.* **28**, 451–457 (2008).

78. Jun, S. Y., Kim, J., Yoon, N., Maeng, L. S. & Byun, J. H. Prognostic potential of cyclin D1 expression in colorectal cancer. *J. Clin. Med.* **12**, 572 (2023).

79. Qasim, B. J., Ali, H. H. & Hussein, A. G. Immunohistochemical expression of PCNA and CD34 in colorectal adenomas and carcinomas using specified automated cellular image analysis system: a clinicopathologic study. *Saudi J. Gastroenterol.* **18**, 268–276 (2012).

80. Melling, N. et al. High Ki67 expression is an independent good prognostic marker in colorectal cancer. *J. Clin. Pathol.* **69**, 209–214 (2016).

81. Liu, Q. et al. Association between Ki67 expression and therapeutic outcome in colon cancer. *Oncol. Lett.* **25**, 272 (2023).

82. Ma, Y. L. et al. Immunohistochemical analysis revealed CD34 and Ki67 protein expression as significant prognostic factors in colorectal cancer. *Med. Oncol.* **27**, 304–309 (2010).

83. Lumachi, F., Orlando, R., Marino, F., Chiara, G. B. & Basso, S. M. Expression of p53 and Ki-67 as prognostic factors for survival of men with colorectal cancer. *Anticancer Res.* **32**, 3965–3967 (2012).

84. Luo, Z. W. et al. Increased expression of Ki-67 is a poor prognostic marker for colorectal cancer patients: a meta analysis. *BMC Cancer* **19**, 123 (2019).

85. Singh, V. et al. Inhibition of interleukin-10 signaling induces microbiota-dependent chronic colitis in apolipoprotein E deficient mice. *Inflamm. Bowel Dis.* **22**, 841–852 (2016).

86. Salvador, P. et al. CD16+ macrophages mediate fibrosis in inflammatory bowel disease. *J. Crohn's Colitis* **12**, 589–599 (2018).

87. Deng, H. et al. Sodium fluoride induces apoptosis in mouse splenocytes by activating ROS-dependent NF-kappaB signaling. *Oncotarget* **8**, 114428–114441 (2017).

88. Zwanziger, D., Rakov, H., Engels, K., Moeller, L. C. & Fuhrer, D. Sex-dependent claudin-1 expression in the liver of euthyroid and hypothyroid mice. *Eur. Thyroid J.* **4**, 67–73 (2015).

89. Zou, J. et al. Fiber-mediated nourishment of gut microbiota protects against diet-induced obesity by restoring IL-22-mediated colonic health. *Cell Host Microbe* **23**, 41–53 e44 (2018).

90. Miranda-Ribera, A. et al. Exploiting the zonulin mouse model to establish the role of primary impaired gut barrier function on microbiota composition and immune profiles. *Front.Immunol.* **10**, 2233 (2019).

91. Holmes, J. L., Van Itallie, C. M., Rasmussen, J. E. & Anderson, J. M. Claudin profiling in the mouse during postnatal intestinal development and along the gastrointestinal tract reveals complex expression patterns. *Gene Expr. Patterns* **6**, 581–588 (2006).

92. Martins, C. S. et al. Clostridioides difficile toxin A-induced Wnt/beta-catenin pathway inhibition is mediated by Rac1 glucosylation. *Front. Microbiol.* **11**, 1998 (2020).

93. Van den Bossche, J. et al. Claudin-1, claudin-2 and claudin-11 genes differentially associate with distinct types of anti-inflammatory macrophages in vitro and with parasite- and tumour-elicited macrophages in vivo. *Scand. J. Immunol.* **75**, 588–598 (2012).

94. Zimmerer, J. M., Pham, T. A., Sanders, V. M. & Bumgardner, G. L. CD8+ T cells negatively regulate IL-4-dependent, IgG1-dominant posttransplant alloantibody production. *J. Immunol.* **185**, 7285–7292 (2010).

95. Tsuboi, K. et al. Autophagy protects against colitis by the maintenance of normal gut microflora and secretion of mucus. *J. Biol. Chem.* **290**, 20511–20526 (2015).

96. An, J. et al. Modulation of pro-inflammatory and anti-inflammatory cytokines in the fat by an aloe gel-based formula, QDMC, is correlated with altered gut microbiota. *Immune Netw.* **21**, e15 (2021).

97. Metruccio, M. M. E. et al. Contributions of MyD88-dependent receptors and CD11c-positive cells to corneal epithelial barrier function against Pseudomonas aeruginosa. *Sci. Rep.* **7**, 13829 (2017).

98. Fernandez-Martin, J. C. et al. Gal3 plays a deleterious role in a mouse model of endotoxemia. *Int. J. Mol. Sci.* **23**, 1170 (2022).

99. Zhang, Y. et al. PTPsigma inhibitors promote hematopoietic stem cell regeneration. *Nat. Commun.* **10**, 3667 (2019).

100. Zerikiotis, S. et al. Synergistic pulmonoprotective effect of natural prolyl oligopeptidase inhibitors in in vitro and in vivo models of acute respiratory distress syndrome. *Int. J. Mol. Sci.* **24**, 14235 (2023).

101. Michel, M., Kaps, L., Maderer, A., Galle, P. R. & Moehler, M. The role of p53 dysfunction in colorectal cancer and its implication for therapy. *Cancers* **13**, 2296 (2021).

102. Rivera, A. D. et al. Drug connectivity mapping and functional analysis reveal therapeutic small molecules that differentially modulate myelination. *Biomed. Pharmacother.* **145**, 112436 (2022).

103. Wang, L. et al. Inhibition of p53 deSUMOylation exacerbates puromycin aminonucleoside-induced apoptosis in podocytes. *Int. J. Mol. Sci.* **15**, 21314–21330 (2014).

104. Chassaing, B. et al. Fecal lipocalin 2, a sensitive and broadly dynamic non-invasive biomarker for intestinal inflammation. *PLoS ONE* **7**, e44328 (2012).

Acknowledgements

Author contributions

V.S. conceived and designed the study. S.T. planned and performed all animal experiments. U.K.G., D.P., and G.V.L. helped with biochemical and histological analysis. A.K.T. and K.S.P. provided critical insights into data interpretation and contributed to manuscript writing. V.S. and S.T. drafted the manuscript. All authors read and approved the final manuscript.

Competing interests

The authors declare no competing interests.

Additional information

Supplementary information The online version contains supplementary material available at https://doi.org/10.1038/s41538-025-00472-1.

Correspondence and requests for materials should be addressed to Vishal Singh.

Reprints and permissions information is available at http://www.nature.com/reprints

Publisher's note Springer Nature remains neutral with regard to jurisdictional claims in published maps and institutional affiliations.